

Methods for Higgs boson production at N³LO*

J. Hoff^{a,1}

^a*Deutsches Elektronen Synchrotron DESY, Platanenallee 6, 15738 Zeuthen, Germany*

Abstract

We discuss methods for the calculation of the total partonic Higgs boson production cross section via gluon fusion and the result for the contribution that stems from two quarks of different flavor in the initial state. Our calculation is exact in the Higgs boson mass and the partonic center-of-mass energy. The result is expressed in terms of iterated integrals, some of which are Harmonic Polylogarithms, whereas others are new iterated integrals. We comment on the methods relevant for the reduction to scalar integrals and new types of function that appear in the final result.

Keywords: Standard Model Higgs boson, total inclusive production cross section, higher order QCD corrections, Harmonic Polylogarithms, iterated integrals

1. Introduction

After the Higgs boson discovery [1, 2], the precise determination of its properties is one of the mayor goals of run II of the LHC. The expected experimental precision in the upcoming years has to be matched by theory predictions. Since the dominant production mechanism for Higgs boson production at the LHC is gluon fusion, QCD corrections are the most sizable ones. In fact, the combined next-to-leading order (NLO) and next-to-next-to-leading order (NNLO) corrections amount to the same size as the leading order (LO) cross section. The NNLO prediction still has to be assigned an uncertainty of about 15% which is to one part due to the parton densities and to another part due to unknown higher orders in the perturbation series of the partonic quantity. Therefore, our interest lies in the computation of the partonic cross section to next-to-next-to-next-to-leading order (N³LO).

Effective field theory

Gluon fusion is a process induced by quark loops and that is dominated by the top quark. Hence, it is reasonable to work within an effective field theory (EFT) where the top quark has been integrated out. In addition to the ordinary five-flavor

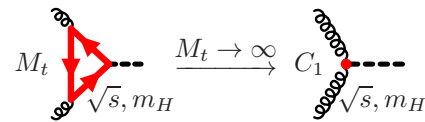


Figure 1: Contraction of the top quark loop corresponds to the transition from the full to the effective theory or to the limit $M_t \rightarrow \infty$. Thick straight lines represent the top quark, dashed lines the Higgs boson, dots its effective coupling and curly lines gluons. Also, we indicated all relevant scales.

Lagrangian of QCD, one has to consider the interaction term

$$\mathcal{L}_{Y,\text{eff}} = -\frac{H}{v}C_1\mathcal{O}_1, \quad \mathcal{O}_1 = \frac{1}{4}G_{\mu\nu}^a G^{a,\mu\nu}, \quad (1)$$

where H denotes the Higgs field, v its vacuum expectation value and C_1 the matching coefficient between full and effective theory. The effective coupling operator \mathcal{O}_1 is composed of the gluon field strength tensor $G_{\mu\nu}$.

The transition from the full to the effective theory can be depicted diagrammatically, see Fig. 1.

The advantage of working within the EFT setup is the smaller number of diagrams and their reduced complexity. There are less loops and less scales that have to be considered simultaneously, as the dependence on the top quark mass M_t is encoded completely in C_1 . EFT diagrams therefore depend only on a single dimensionless variable $x = m_H^2/s$ which is the squared ratio of the Higgs boson mass m_H and the partonic center-of-mass energy \sqrt{s} .

For Higgs boson production to N³LO, the finite

*Talk given at 18th International Conference in Quantum Chromodynamics (QCD 15, 30th anniversary), 29 June - 3 July 2015, Montpellier - FR

Email address: jens.hoff@desy.de (J. Hoff)

¹Speaker, Corresponding author.

$$\begin{aligned}
& \int d\Pi_1 \left| \text{[Tree-level diagram]} + \text{[One-loop diagram]} + \dots \right|^2 \\
& + \int d\Pi_2 \left| \text{[One-loop diagram]} + \text{[Two-loop diagram]} + \dots \right|^2 \\
& + \int d\Pi_3 \left| \text{[Two-loop diagram]} + \text{[Three-loop diagram]} + \dots \right|^2 + \dots \\
& = \text{[Tree-level interference]} + \text{[One-loop interference]} + \dots + \text{[Two-loop interference]} + \dots \\
& \quad + \text{[Cut diagrams]} + \dots + \text{[Cut diagrams]} + \dots
\end{aligned}$$

Figure 2: Illustration of the optical theorem up to NNLO, see the main text for details. Apart from the notation in Fig. 1, wiggly lines represent cuts.

matching coefficient C_1 is needed to four-loop order, see Refs. [3–5]. The renormalization of C_1 is described in Ref. [6] and can be expressed via the renormalization constant of α_s which is also itself needed to three-loop order, see Refs. [7, 8].

Optical theorem and Cutkosky rules

The computation of higher order corrections to the cross section of a process requires taking into account virtual (additional loops) and real (additional final state particles) contributions. Instead of considering different phase spaces for the final states, one can employ the optical theorem which relates the total cross section to the imaginary part of the forward scattering amplitude. Symbolically:

$$\begin{aligned}
\sigma(i \rightarrow f) & \sim \sum_f \int d\Pi_f |\mathcal{M}(i \rightarrow f)|^2 \\
& \sim \text{Im} \mathcal{M}(i \rightarrow i), \quad (2)
\end{aligned}$$

where σ denotes the total cross section for an initial state i to result in a collection of final states f and \mathcal{M} stands for the matrix element for a transition between states (which are identical for forward scattering). The Cutkosky rules in turn relate different contributions to the imaginary part of an amplitude to specific sets of propagators which are set on-shell and thereby “cut”.

Figure 2 exemplifies this technique up to NNLO. The left-hand side shows the phase space integrals over squared production amplitudes for the Higgs boson with up to two additional partons. The right-hand side shows the corresponding interference diagrams where the cut-line is equivalent to a phase space. Note, the last two diagrams are different cuts of the same amplitude. This demonstrates the validity just to consider all relevant cuts of the forward scattering amplitude.

Working in forward scattering kinematics simplifies the calculation. The optical theorem allows for common treatment of loop and phase space integrals. Thus, the calculation of imaginary parts has to be performed only for a relatively small set of “master integrals” (the integrals remaining after application of integration-by-parts identities with Laporta’s algorithm). This approach was first used in Ref. [9] for the NNLO computation of Higgs production. On the other hand, within this method more diagrams with more loops have to be computed and one has only access to a total inclusive cross section, at least in its naïve application.

Existing results

Let us give a listing of available results related to the Higgs boson production cross section. In Fig. 3 we give sample diagrams for the contributions from different cuts at N³LO.

- The LO cross section (with exact dependence on M_t) was computed already in the seventies, see Refs. [10–13].
- NLO corrections (also exact in M_t) are available for almost twenty years, see Refs. [14, 15].
- NNLO corrections were first calculated within the EFT in Refs. [9, 16, 17]. Note that in Ref. [16] the soft expansion $x \rightarrow 1$ to high orders was used where already the third order proved to be valid within an error of $\mathcal{O}(1\%)$.
- In Refs. [18–23] the expansion in m_H^2/M_t^2 was performed to assess the error within the EFT framework which turned out to be of $\mathcal{O}(1\%)$.
- Combining three-loop splitting functions [24, 25] with partonic cross sections to NNLO expanded to higher orders in the dimensional regulator [23, 26], convolution integrals and infrared counterterms could be presented in [27–29]. In Ref. [28] the N³LO scale variation was constructed and found to be of $\mathcal{O}(2\% - 8\%)$.

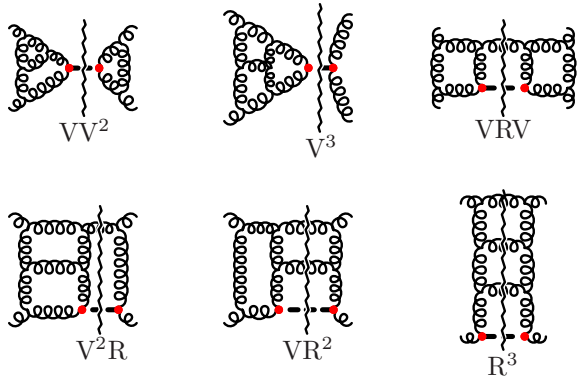


Figure 3: Different types of cut contributions at $N^3\text{LO}$. The notation is as in Fig. 2, “V” stands for virtual and “R” for real in order to abbreviate contributions.

- The three-loop gluon form factor was computed in Refs. [30, 31] which gives the VV^2 and V^3 contributions.
- For VRV and V^2R contributions (both exact in x), see Refs. [32, 33] and Refs. [34, 35], respectively.
- For VR^2 and R^3 contributions (both as expansion in $x \rightarrow 1$), see Refs. [36–38] and Ref. [39], respectively. In Refs. [38] more than thirty terms in the soft expansion were reached for the total cross section which is sufficient for phenomenological applications.
- In Refs. [40, 41] the qq' -channel was considered and exact results could be obtained for its VR^2 and R^3 contributions.

2. Computational techniques

Generally, there is a steep raise in complexity when going to higher loop orders in a specific process. Here, there is only 1 diagram at LO, 50 at NLO, 2946 at NNLO and 174938 at $N^3\text{LO}$. The corresponding integrals are classified in “topologies” or Feynman integral families which are then subject to a reduction algorithm resulting in a set of master integrals. For the real corrections to Higgs boson production 1 topology is needed at NLO, 11 at NNLO and more than 100 at $N^3\text{LO}$. The number of master integrals is 1 at NLO, 20 at NNLO and more than 100 at $N^3\text{LO}$.

Our computational setup is highly automated. First, we use QGRAF [43] to generate and a private

filter [44] to select all relevant Feynman diagrams. We perform two independent calculations, using either the program `exp` [45, 46] or `reg` to map diagrams to topologies. The reduction to scalar integrals is then performed with `FORM` [47, 48]. The reduction to master integrals is done with `rows` (an in-house Laporta algorithm) and `FIRE` [49]. The reduction tables can reach a size of up to ten gigabytes.

The private code `TopoID` [44, 50] is used to provide input in an automatic fashion for the aforementioned steps. Based on the appearing diagrams, we define a topology as set of propagators allowing for permutations or contractions of propagators and (linear) transformations of loop momenta. `TopoID` can also handle topologies with linearly dependent propagators which are needed to map all appearing diagrams. For the partial fractioning relations and the decomposition into topologies with linearly independent propagators `FORM` code is generated. Since the momentum space representation of topologies is ambiguous, we employ the Feynman representation in a unique form to identify duplicate topologies and also to find a minimal basis of master integrals in the very end. This form of the Feynman representation is also used to obtain all possible symmetries of topologies which is an enormous aid in the Laporta reduction. Moreover, `TopoID` is able to handle cuts of Feynman diagrams in the sense that all possible ways are detected to set propagators on-shell giving rise to an imaginary part. For details we refer the interested reader to [44].

The master integrals are calculated using the technique of canonical differential equations (DEQs), see e.g. Ref. [42]. In general, one obtains a coupled system of linear first-order DEQs for the master integrals. This system is generated by applying the derivative in a kinematic invariant or mass on the integrand of a master integral and using the reduction procedure subsequently. We refrain from giving details on the computation of the soft limit $x \rightarrow 1$ which is used as boundary condition and refer instead to Ref. [41].

In the last few years Henn [42], advertised a specific form of DEQs which can be reached via a basis transformation of the master integrals and cast in the form

$$\frac{d}{dx} m_i(x, \epsilon) = \epsilon A_{ij}(x) m_j(x, \epsilon), \quad (3)$$

where m_i is a vector of master integrals, A_{ij} the fun-

damental matrix of the DEQs, x a scaleless variable and $d = 4 - 2\epsilon$ the number of spacetime dimensions. The appeal of this form lies in the factorization of the dependence on the dimensional regulator ϵ and the kinematics. In this form the system can be solved order by order in ϵ and one can immediately read off the so-called “alphabet”, the set of integration kernels, of the iterated integrals that pose the solutions.

Up to NNLO all integrals can be represented as Harmonic Polylogarithms (HPLs), denoted $H_{\vec{w}}(x)$, which are defined as follows:

$$H_{\vec{w}}(x) = \int_0^x dx' f_{w_1}(x') H_{\vec{w}_{n-1}}(x'), \quad (4)$$

$$f_0(x) = \frac{1}{x}, \quad f_1(x) = \frac{1}{1-x}, \quad f_{-1}(x) = \frac{1}{1+x},$$

where $\vec{w} = (w_1, \vec{w}_{n-1})$ is the vector of n weights and the f_i are the integration kernels. On N³LO, as we will see in Section 3, HPLs are not sufficient anymore and the class of functions needs to be extended.

3. The qq' -channel

There are 220 diagrams to be calculated in the qq' -channel which we chose to classify into 17 topologies, see Fig. 4. Some of the integrals of only one of these topologies (the third in the first row if Fig. 4) could not be solved in terms of HPLs only. In that case the extended alphabet compared to Eq. (4) yields also the “letters”

$$f_{-4} = \frac{1}{1+4x}, \quad f_{s4} = \frac{1}{x} \left(\frac{1}{\sqrt{1+4x}} - 1 \right). \quad (5)$$

Note that all integrals giving solutions of this kind can be traced back to the common graph in Fig. 5. We refrain from giving any explicit results here, instead we refer to Refs. [41, 51].

4. Conclusion

We described the computation of a contribution to the partonic cross section for Higgs boson production via gluon fusion to N³LO. That is, the subprocess initiated by two quarks of different flavour. We obtained analytic results with exact dependence on the Higgs boson mass and the partonic center-of-mass energy. New types of iterated integrals beyond Harmonic Polylogarithms appear in the final expression.

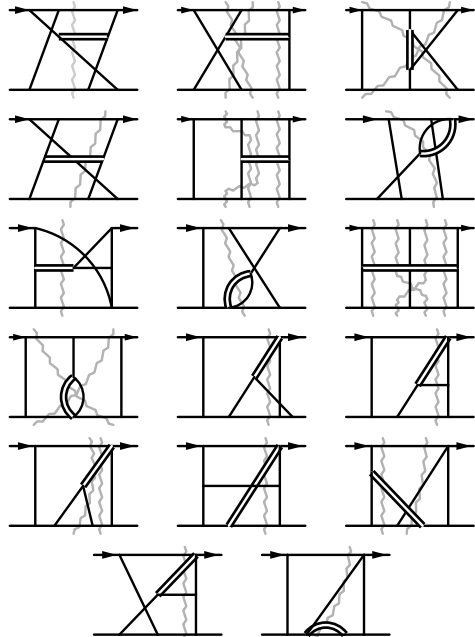


Figure 4: The 17 topologies used for the calculation of the qq' -channel. Plain lines are massless and double lines massive. Arrows indicate the planar flow of external momenta and gray wiggly lines the three- and four-particle cuts.

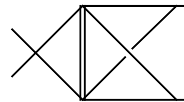


Figure 5: Common graph of all integrals that give rise to functions beyond HPLs.

This work represents an important step towards an exact result for all N³LO contributions to Higgs boson production. To date only an expansion around the soft limit is available from the literature [36–38, 52] which is, however, sufficient for phenomenology. Performing an expansion of our result around the threshold, we find for leading logarithms agreement with the results from Ref. [52].

5. Acknowledgments

We would like to thank our collaborators C. Anzai, A. Hasselhuhn, M. Höschele, W. Kilgore, M. Steinhauser and T. Ueda. Parts of this work were supported by the European Commission through contract PITN-GA-2012-316704 (HIG-GSTOOLS).

References

- [1] G. Aad *et al.* [ATLAS Collaboration], *Phys. Lett. B* **716**, 1 (2012) [arXiv:1207.7214 [hep-ex]].
- [2] S. Chatrchyan *et al.* [CMS Collaboration], *Phys. Lett. B* **716**, 30 (2012) [arXiv:1207.7235 [hep-ex]].
- [3] K. G. Chetyrkin, B. A. Kniehl and M. Steinhauser, *Nucl. Phys. B* **510** (1998) 61 [hep-ph/9708255].
- [4] Y. Schröder and M. Steinhauser, *JHEP* **0601** (2006) 051, arXiv:hep-ph/0512058.
- [5] K. G. Chetyrkin, J. H. Kühn and C. Sturm, *Nucl. Phys. B* **744** (2006) 121, arXiv:hep-ph/0512060.
- [6] V. P. Spiridonov, IYaI-P-0378.
- [7] O. V. Tarasov, A. A. Vladimirov and A. Y. Zharkov, *Phys. Lett. B* **93** (1980) 429.
- [8] S. A. Larin and J. A. M. Vermaseren, *Phys. Lett. B* **303** (1993) 334 [hep-ph/9302208].
- [9] C. Anastasiou and K. Melnikov, *Nucl. Phys. B* **646**, 220 (2002) [hep-ph/0207004].
- [10] F. Wilczek, *Phys. Rev. Lett.* **39** (1977) 1304.
- [11] J. R. Ellis, M. K. Gaillard, D. V. Nanopoulos and C. T. Sachrajda, *Phys. Lett. B* **83** (1979) 339.
- [12] H. M. Georgi, S. L. Glashow, M. E. Machacek and D. V. Nanopoulos, *Phys. Rev. Lett.* **40** (1978) 692.
- [13] T. G. Rizzo, *Phys. Rev. D* **22** (1980) 178 [Addendum-*ibid.* **D 22** (1980) 1824].
- [14] S. Dawson, *Nucl. Phys. B* **359** (1991) 283.
- [15] M. Spira, A. Djouadi, D. Graudenz and P. M. Zerwas, *Nucl. Phys. B* **453** (1995) 17, arXiv:hep-ph/9504378.
- [16] R. V. Harlander and W. B. Kilgore, *Phys. Rev. Lett.* **88** (2002) 201801, arXiv:hep-ph/0201206.
- [17] V. Ravindran, J. Smith and W. L. van Neerven, *Nucl. Phys. B* **665** (2003) 325, arXiv:hep-ph/0302135.
- [18] R. V. Harlander and K. J. Ozeren, *Phys. Lett. B* **679** (2009) 467 [arXiv:0907.2997 [hep-ph]].
- [19] A. Pak, M. Rogal and M. Steinhauser, *Phys. Lett. B* **679** (2009) 473 [arXiv:0907.2998 [hep-ph]].
- [20] R. V. Harlander and K. J. Ozeren, *JHEP* **0911** (2009) 088 [arXiv:0909.3420 [hep-ph]].
- [21] A. Pak, M. Rogal and M. Steinhauser, *JHEP* **1002**, 025 (2010) [arXiv:0911.4662 [hep-ph]].
- [22] R. V. Harlander, H. Mantler, S. Marzani and K. J. Ozeren, *Eur. Phys. J. C* **66** (2010) 359 [arXiv:0912.2104 [hep-ph]].
- [23] A. Pak, M. Rogal and M. Steinhauser, *JHEP* **1109** (2011) 088 [arXiv:1107.3391 [hep-ph]].
- [24] S. Moch, J. A. M. Vermaseren and A. Vogt, *Nucl. Phys. B* **688** (2004) 101 [hep-ph/0403192].
- [25] A. Vogt, S. Moch and J. A. M. Vermaseren, *Nucl. Phys. B* **691** (2004) 129 [hep-ph/0404111].
- [26] C. Anastasiou, S. Buehler, C. Duhr and F. Herzog, *JHEP* **1211** (2012) 062 [arXiv:1208.3130 [hep-ph]].
- [27] M. Höschele, J. Hoff, A. Pak, M. Steinhauser and T. Ueda, *Phys. Lett. B* **721** (2013) 244 [arXiv:1211.6559 [hep-ph]].
- [28] S. Buehler and A. Lazopoulos, *JHEP* **1310** (2013) 096 [arXiv:1306.2223 [hep-ph]].
- [29] M. Höschele, J. Hoff, A. Pak, M. Steinhauser and T. Ueda, *Comput. Phys. Commun.* **185** (2014) 528 [arXiv:1307.6925].
- [30] P. A. Baikov, K. G. Chetyrkin, A. V. Smirnov, V. A. Smirnov and M. Steinhauser, *Phys. Rev. Lett.* **102** (2009) 212002 [arXiv:0902.3519 [hep-ph]].
- [31] T. Gehrmann, E. W. N. Glover, T. Huber, N. Iklizlerli and C. Studerus, *JHEP* **1006** (2010) 094 [arXiv:1004.3653 [hep-ph]].
- [32] C. Anastasiou, C. Duhr, F. Dulat, F. Herzog and B. Mistlberger, *JHEP* **1312** (2013) 088 [arXiv:1311.1425 [hep-ph]].
- [33] W. B. Kilgore, *Phys. Rev. D* **89** (2014) 073008 [arXiv:1312.1296 [hep-ph]].
- [34] F. Dulat and B. Mistlberger, arXiv:1411.3586 [hep-ph].
- [35] C. Duhr, T. Gehrmann and M. Jaquier, arXiv:1411.3587 [hep-ph].
- [36] C. Anastasiou, C. Duhr, F. Dulat, E. Furlan, T. Gehrmann, F. Herzog and B. Mistlberger, *Phys. Lett. B* **737** (2014) 325 [arXiv:1403.4616 [hep-ph]].
- [37] Y. Li, A. von Manteuffel, R. M. Schabinger and H. X. Zhu, arXiv:1412.2771 [hep-ph].
- [38] C. Anastasiou, C. Duhr, F. Dulat, F. Herzog and B. Mistlberger, arXiv:1503.06056 [hep-ph].
- [39] C. Anastasiou, C. Duhr, F. Dulat and B. Mistlberger, *JHEP* **1307** (2013) 003 [arXiv:1302.4379 [hep-ph]].
- [40] M. Höschele, J. Hoff and T. Ueda, *JHEP* **1409** (2014) 116 [arXiv:1407.4049 [hep-ph]].
- [41] C. Anzai, A. Hasselhuhn, M. Höschele, J. Hoff, W. Kilgore, M. Steinhauser and T. Ueda, *JHEP* **1507**, 140 (2015) [arXiv:1506.02674 [hep-ph]].
- [42] J. M. Henn, *Phys. Rev. Lett.* **110** (2013) 25, 251601 [arXiv:1304.1806 [hep-th]].
- [43] P. Nogueira, *J. Comput. Phys.* **105** (1993) 279.
- [44] J. Hoff, “Methods for multiloop calculations and Higgs boson production at the LHC”, Dissertation, KIT, 2015.
- [45] R. Harlander, T. Seidensticker and M. Steinhauser, *Phys. Lett. B* **426** (1998) 125 [hep-ph/9712228].
- [46] T. Seidensticker, hep-ph/9905298.
- [47] J. A. M. Vermaseren, math-ph/0010025.
- [48] J. Kuipers, T. Ueda, J. A. M. Vermaseren and J. Vollinga, *Comput. Phys. Commun.* **184** (2013) 1453 [arXiv:1203.6543 [cs.SC]].
- [49] A. V. Smirnov, *Comput. Phys. Commun.* **189** (2014) 182 [arXiv:1408.2372 [hep-ph]].
- [50] J. Grigo and J. Hoff, *PoS LL* **2014** (2014) 030 [arXiv:1407.1617 [hep-ph]].
- [51] <http://www.ttp.kit.edu/Progdata/ttp15/ttp15-019/>
- [52] C. Anastasiou, C. Duhr, F. Dulat, E. Furlan, T. Gehrmann, F. Herzog and B. Mistlberger, arXiv:1411.3584 [hep-ph].